Label free detection of Prostate Specific Antigen at a screen printed immunosensor modified with a nano-structured gold layer

CL-170790 Received: August 29, 2017 | Accepted: September 22, 2017 | Web Released: November 1, 2017

Label-free Detection of Prostate Specific Antigen at a Screen-printed Immunosensor Modified with a Nanostructured Gold Layer

Sean Rawlinson,* Prosper Kanyong, Aaron McConville, John-Joe Fearon, James A. D. McLaughlin, and James Davis
School of Engineering, Ulster University, Jordanstown, Northern Ireland, BT37 0QB

(E-mail: Rawlinson-S@email.ulster.ac.uk)

The development of a disposable immunosensor based on a hybrid gold–carbon screen-printed electrode array is described. The electrodeposition of gold is shown to lead to a field of nanocrystals that facilitates antibody immobilization and enhances electron transfer. A label-free analysis protocol based on ferrocyanide has been developed for the detection of Prostate Specific Antigen in the fg mL^{-1} range.

Keywords: Prostate specific antigen (PSA) | Disposable immunosensor | Au–carbon screen-printed electrode

Prostate cancer (PCa) is a significant cause of morbidity and mortality and the most common cancer in men in Europe, North America, and some parts of Africa.[1–3] The disease can be particularly problematic from an observational diagnostic perspective as symptoms may not become apparent until the cancer is in its advanced stages. A second issue arises from the fact that there can be considerable reluctance on the part of the patient to actively request medical advice.[4] Even where help is sought, clinical assessment can be ambiguous as many of the complaints are seldom specific to PCa and can easily be attributed to a host of other non-cancerous conditions such as infection or inflammation. There are many issues that can impede early diagnosis and, all too often, the cancer is not detected until the cancer has spread.[4] The need for rapid screening diagnostics for PCa has long been recognized and there have been some measures to proactively screen those sectors of the populace who are deemed to be "at risk". Prostate cancer incidence is strongly linked to age and seldom diagnosed in those younger than 50 years. It has been reported that in the UK (between 2009 and 2011 some 36% of new cases were diagnosed in older men (>75 years) with under 50s accounting for only 1%.[5]

The concentration of Prostate Specific Antigen (PSA) in serum is presently the principal screening biomarker for PCa and has use in the staging and post therapy monitoring of the disease.[6,7] It has been established that the majority of men diagnosed with PCa will have clinically impalpable carcinoma with elevated levels of serum PSA in the range of 2.5–10.0 ng mL^{-1}.[8] There is however a positive predictive value (PPV) of elevated serum PSA for the detection of PCa but this largely depends on the definition of an optimal upper limit of "normal" PSA levels.[6] The PPV for histological diagnosis of PCa with serum PSA >4 ng mL^{-1} has been reported to lie between 31–51%.[9] At high serum PSA levels (>10 ng mL^{-1}), the probability of disease detection is ca. 60%. However, as most men present with levels lower than 10 ng mL^{-1} there is a continuing challenge to improve the PPV of serum PSA, In response, various adaptations to the basic PSA assay have been developed and include: proPSA, PSA doubling time (PSADT), age-specific PSA, PSA velocity (PSAV, rate of change of PSA levels over time), PSA density (PSAD = serum PSA/ultrasound volume of the prostate gland), free PSA (fPSA), percent free PSA (%fPSA), complexed PSA, and benign PSA (BPSA).[10–12] A detailed description of these assays is provided elsewhere[4] but irrespective of the assay type: the central limitation is that the analysis is done within a central laboratory. There remains a pressing need to provide much more routine screening within the primary care sector and it is little surprise to find that the sensor community continues to explore the development of PSA technologies.

Some of more recent developments in PSA immunosensing technologies include field effect devices,[13,14] microbalances and nanoresonators[15,16] but most activity is directed towards modified electrode systems: typically employing nanoparticles and 2D materials.[17–22] The use of screen-printed electrode (SPE) systems is arguably the more commercially viable and provides a disposable format which is particularly suited towards a clinical environment. The aim of the present communication has been to explore the development of a modified SPE capable of detecting PSA within the desired clinical range and which could possess sufficient versatility to be expanded to the other PSA assay variations noted earlier. The basic approach to the fabrication of the sensing strip is highlighted in Figure 1 and consists of a series of surface modifications.

The electrodeposition of the gold sublayer is a critical component as it provides the means through which to anchor the antibody and, it was envisaged, would enhance the response to the redox probe. The latter is an important consideration as the

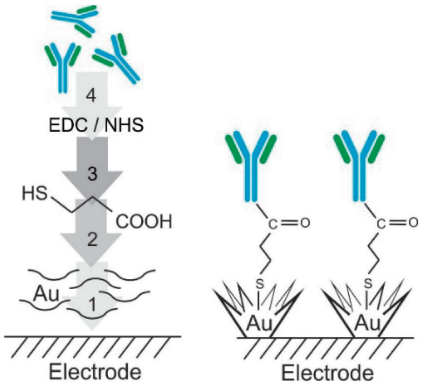

Figure 1. Assembly steps in production of the nanocrystalline Au–carbon immunosensor. 1) Electrodeposition of Au onto carbon screen-printed electrode. 2) Functionalization of Au layer with mercaptopropionic acid (MPA). 3) Activation of carboxy groups with 1-ethyl-3-(3-dimethylaminopropyl)carbodiimide hydrochloride (EDC) and *N*-hydroxysuccinimide (NHS). 4) Coupling of PSA antibody to modified electrode.

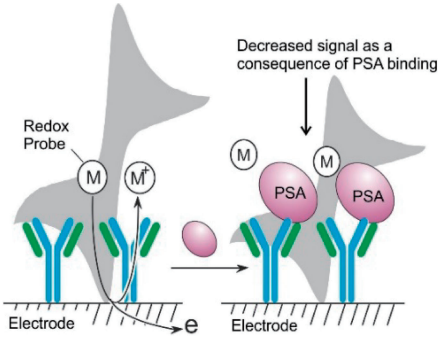

Figure 2. Schematic highlighting the effect of antigen binding on the cyclic voltammetric response to a generic mediator (M).

analytical signal is determined through the oxidation of ferrocyanide at the underlying substrate. Ferrocyanide was chosen on the basis of its reversible electrode behavior at gold and low oxidation potential which could aid discrimination from common electroactive interferences such as urate and ascorbate. Other mediators with lower oxidation potentials such as riboflavin have been used in immunosensors[23] but these can fall foul of oxygen interference. The general label-free detection methodology is highlighted in Figure 2. The binding of the PSA to the immobilized antibody reduces the access of the ferrocyanide probe to the electrode and consequently there is a reduction in the current. In the present paper, cyclic voltammetry is used to probe the antigen–antibody interactions.

All chemicals were obtained from Sigma-Aldrich, were the highest grade available and were used without further purification. Electrochemical analysis was carried out using a VSP-300 Multichannel Potentiostat/Galvanostat/EIS (Bio-Logic Science Instruments, EC-Lab Ltd.) with a standard three-electrode configuration with a carbon screen-printed working electrode, a platinum wire counter electrode, and a standard silver/silver chloride (3 M NaCl, BAS Technicol UK) reference electrode. All measurements were conducted at 22 ± 2 °C.

Screen-printed electrodes (SPEs) were fabricated using a DEK 240 Manual Screen Printing Machine using a stainless-steel screen mesh and commercial graphite ink (Gwent Electronic Materials (GEM) Product code: C205010697). Initially, the base of the SPE was printed onto a Valox substrate which was cured at 70 °C for 90 min. To define the working area, a polymeric dielectric material (GEM Product code: D2071120P1) was then screen-printed onto the cured SPE. A JEOL JSM-6010 Plus scanning electron microscope (SEM) was used to characterize the surface morphology of the carbon sensors and a representative micrograph of the carbon print morphology and the nanoporous nature of the deposit is highlighted in Figure 3A. The screen-printed array is detailed in Figure 3B along with the surface roughness results obtained from the application of a DEKTAK XT Stylus Profiler (Bruker) system. The results from three electrodes are compared in Figure 3B and it can be seen that the typical thickness of the print is of the order of 20 micron.

It has become relatively common to electrochemically anodise carbon composite electrodes in order to elicit improved electrochemical behavior.[24,25] The electro-oxidation (+2 V, 0.1 M NaOH) typically increases exfoliation of the carbon particles—generating more edge plane sites and increases the

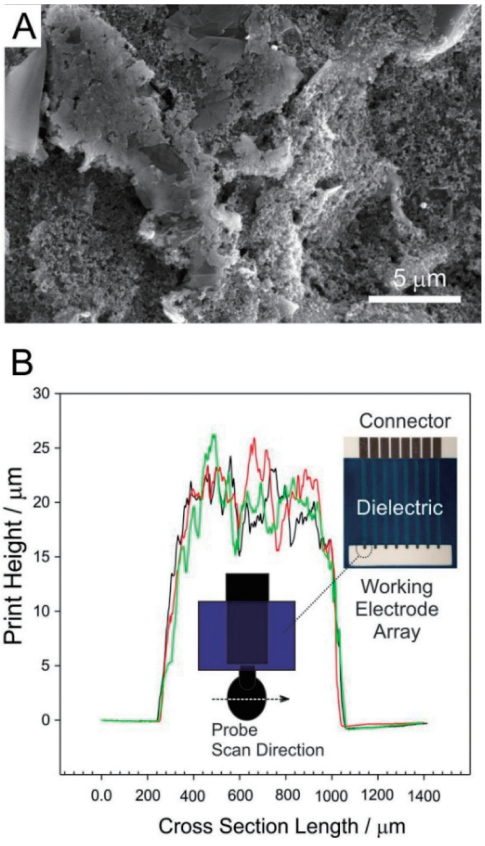

Figure 3. A) Scanning electron micrograph of the carbon surface on the working electrode disc. Inset: Digital images of the complete printed array and the working electrodes. B) DEKTAK surface profile comparison of three working electrodes.

populations of various oxygen functional groups.[24,25] This process was also instituted here where it has been found that the unmodified screen-printed electrodes typically exhibit poor electrochemical behavior with large overpotentials necessary to obtain any significant analytical responses.[24]

The electrodes were further modified through the electrodeposition of a gold layer. This was achieved through employing cyclic voltammetry whereby the pre-anodized screen-printed electrode was immersed in a gold(III) chloride solution (6 mM $NaAuCl_4$, 0.1 M HNO_3) and scanned between −0.2 and 1.6 V for 20 scans at 0.1 V s^{-1}. The electrodes were then removed, rinsed, and dried. Scanning electron micrographs of the gold deposit are shown in Figure 4. The initial carbon deposit shown in Figure 3A details a highly microporous morphology. The electrodeposition of the gold however appears to decorate the carbon substructure with a field of discrete nanocrystal deposits.

The final stage in the sensor assembly involved the immobilization of the PSA antibodies. The gold–carbon SPE was first immersed into a solution of 3-mercaptopropionic acid (MPA) (10 mM, deionized water) for one hour, rinsed and then placed in a solution containing equimolar 1-ethyl-3-(3-dimethylaminopropyl)carbodiimide hydrochloride and *N*-hydroxysuccinimide (0.04 M) for 30 min. The electrodes were removed and spotted with a 0.2 mg mL^{-1} solution of the PSA antibody and left overnight (ca. 18 h). The electrodes were thoroughly rinsed

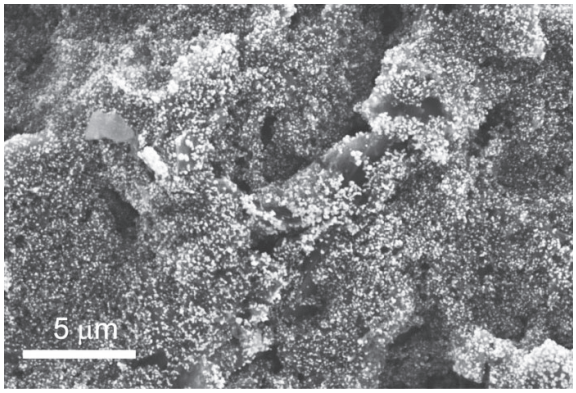

Figure 4. Scanning electron micrograph of the carbon surface after the electrodeposition of the gold layer.

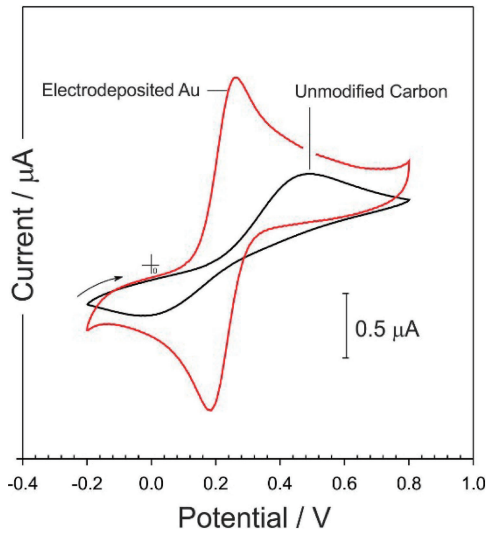

Figure 5. Cyclic voltammograms detailing the response of a carbon screen-printed electrode towards ferrocyanide (2 mM, 0.1 M KCl, 50 mV s^{-1}) before and after the electrodeposition of Au. Scan rate: 50 mV s^{-1}.

with phosphate buffered saline (PBS) and then left in a solution of 1% bovine serum albumin for one hour to block any remaining sites and then rinsed with PBS. This is a critical component in the overall assembly process as the presence of unblocked areas on the electrode surface and the easy access of ferrocyanide could come to dominate the analytical signal and reduce the sensitivity to antigen binding.[26,27]

Cyclic voltammograms comparing the response of the screen-printed sensor to ferrocyanide before and after the electrodeposition of gold are detailed in Figure 5. The bare, unmodified carbon exhibits relatively poor performance in terms of the oxidation of ferrocyanide (2 mM, 0.1 M KCl) with the peak observed at +0.457 V. Similarly, the reduction process is poor with a peak separation of more than 400 mV. This is attributed to the carbon particles within the ink formula consisting of predominantly basal planes.[24,25] The response to ferrocyanide after the electro-deposition of the gold stands in marked contrast with superior peak definition. The peak magnitude of the gold SPE is more than double that of the bare

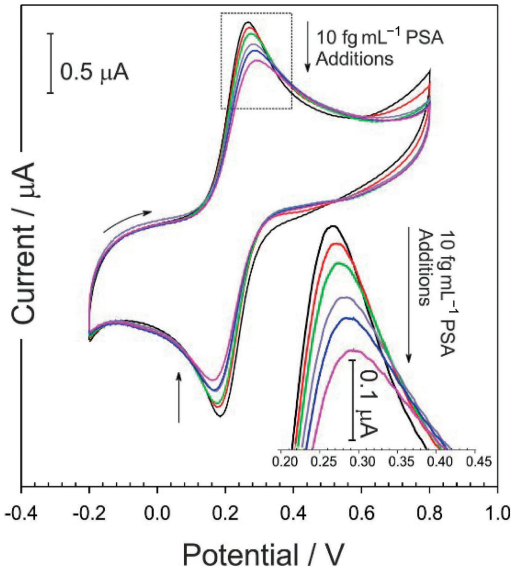

Figure 6. Cyclic voltammograms detailing the response of an antibody-modified gold–carbon screen-printed electrode towards ferrocyanide (2 mM) before and after additions of PSA (10 fg mL^{-1}). Scan rate: 50 mV s^{-1}.

carbon with increased reversibility of the redox system where the peak separation has decreased to 71 mV. The acquisition of a sharp unambiguous peak process at a low operating potential is a critical factor for the successful deployment of the methodology advocated in Figure 2. In the case of the unmodified carbon electrode, the overpotential required before any appreciable oxidation current is observed would inevitably induce the oxidation of other matrix components—lead to signal amplification and compromise the interpretation of the response. The oxidation peak observed with the gold-modified system (+0.257 V) markedly reduces the likelihood of such interference.

Surface modification of the gold with a sequence of protein coupling agents: MPA/EDC/NHS and the PSA antibody leads only to minor modification of the electrode response as indicated in Figure 6 where the ferrocyanide oxidation and reduction peaks are still clearly visible. The addition of aliquots of PSA (10 fg mL^{-1}, 0.01 M PBS) lead to a successive decrease in the oxidation peak height consistent with the label-free detection methodology highlighted in Figure 2.

The electrode response was found to be consistent with the work of other research groups employing cyclic voltammetry for the identification and quantification of antigen binding events.[22] The response observed here however is markedly more sensitive (LOD: 4.7 fg mL^{-1} based on $3S_b$) than many of the current approaches to PSA detection and can be attributed to the high activity of the underpinning gold layer for both the immobilization of the antibody and in facilitating the response to the redox probe. The reproducibility of the system is highlighted in Figure 7 where the responses to femtogram amounts of the PSA are detailed for three individual electrode systems within the printed array shown in Figure 3B.

While the intrabatch reproducibility highlighted here is clearly promising, the nature of the steps involved in the manufacture of the strips would require more elaborate calibration processes before clinical deployment. The label-free

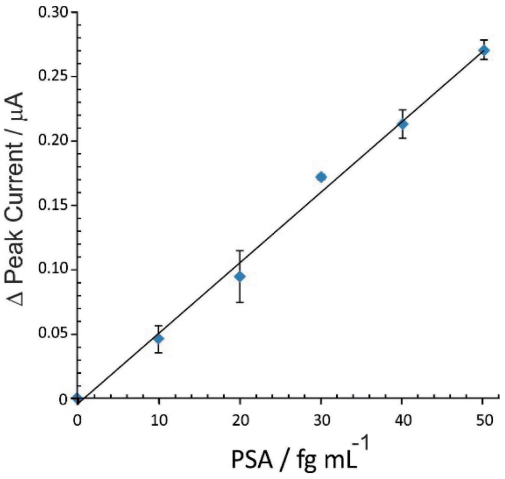

Figure 7. Calibration data for three immunosensors with the analytical response extracted from the change in ferrocyanide oxidation peak upon exposure to PSA (10 fg mL^{-1}).

approach advocated here does however offer a much simpler operational protocol which avoids the multiple washing steps associated with conventional sandwich assay systems.[20–22] A large variety of nanoparticles have been widely used in the development of electrochemical immunosensors with the more recent exploiting Au,[17–19] Pt-Cu,[18] SiO_2,[20] TiO_2,[21] and MoS_2.[22] Such moieties can however create some issues when considering the development of disposable arrays and attempting to control their immobilization at small dimension sensors. Electrodeposition can enable spatial control over the deposition process and, as indicated in this communication, enables the seeding of the electrode surface with highly active gold nanostructures. It could be envisaged that the adoption of square wave voltammetric detection and the translation of the system to smaller geometries where reductions in signal background could herald further gains in sensitivity but these systems invariably come at the expense of greater instrumentation requirements in terms of manufacture and clinical operation. The system adopted here enables rapid manufacture using conventional and accessible technologies. Moreover, the immobilization process is generic and, it could be envisaged, the printed array could ultimately be used to screen for a range of biomarkers and facilitate multiparametric analysis.

The authors thank the Department of Learning Northern Ireland (USI:035) for supporting this work.

References and Notes

1 J. Ferlay, H.-R. Shin, F. Bray, D. Forman, C. Mathers, D. M. Parkin, *Int. J. Cancer* **2010**, *127*, 2893.
2 Population Reference Bureau, 2014 World Population Data Sheet. www.prb.org; August **2014**.
3 Prostate cancer, estimated incidence, mortality and prevalence worldwide 2012, using data from GLOBOCAN 2012, IARC, http://globocan.iarc.fr/Pages/fact_sheets_cancer.aspx.
4 P. Kanyong, S. Rawlinson, J. Davis, *J. Cancer* **2016**, *7*, 523.
5 Cancer Research UK 2015, http://www.cancerresearchuk.org/cancer-info/cancerstats/keyfacts/prostate-cancer.
6 H. Lilja, D. Ulmert, A. J. Vickers, *Nat. Rev. Cancer* **2008**, *8*, 268.
7 P. A. Humprey, G. L. Androiole, *Mol. Med.* **2010**, *107*, 107.
8 I. M. Thompson, D. K. Pauler, P. J. Goodman, C. M. Tangen, M. S. Lucia, H. L. Parnes, L. M. Minasian, L. G. Ford, S. M. Lippman, E. D. Crawford, J. J. Crowley, C. A. Coltman, *N. Engl. J. Med.* **2004**, *350*, 2239.
9 A. V. D'Amico, M.-H. Chen, K. A. Roehl, W. J. Catalona, *N. Engl. J. Med.* **2004**, *351*, 125.
10 W. J. Catalona, A. W. Partin, K. M. Slawin, M. K. Brawer, R. C. Flanigan, A. Patel, J. P. Richie, J. B. deKernion, P. C. Walsh, P. T. Scardino, P. H. Lange, E. N. P. Subong, R. E. Parson, G. H. Gasior, K. G. Loveland, P. C. Southwick, *JAMA* **1998**, *279*, 1542.
11 S. D. Mikolajczyk, L. S. Millar, T. J. Wang, H. G. Rittenshouse, L. S. Marks, W. T. Song, T. M. Wheeler, K. M. Slawin, *Cancer Res.* **2000**, *60*, 756.
12 V. K. Tamboli, N. Bhalla, P. Jolly, C. R. Bowen, J. T. Taylor, J. L. Bowen, C. J. Allender, P. Estrela, *Anal. Chem.* **2016**, *88*, 11486.
13 N. Gao, T. Gao, X. Yang, X. Dai, W. Zhou, A. Zhang, C. M. Lieber, *Proc. Natl. Acad. Sci. U.S.A.* **2016**, *113*, 14633.
14 Z. Han, Y. Wang, X. Duan, *Anal. Chim. Acta* **2017**, *964*, 170.
15 L. Su, L. Zou, C.-C. Fong, W.-L. Wong, F. Wei, K.-Y. Wong, R. S. S. Wu, M. Yang, *Biosens. Bioelectron.* **2013**, *46*, 155.
16 M. Li, P. Wang, F. Li, Q. Chu, Y. Li, Y. Dong, *Biosens. Bioelectron.* **2017**, *87*, 752.
17 Y. Wei, X. Li, X. Sun, H. Ma, Y. Zhang, Q. Wei, *Biosens. Bioelectron.* **2017**, *94*, 141.
18 L. Jiao, Z. Mu, L. Miao, W. Du, Q. Wei, H. Li, *Microchim. Acta* **2017**, *184*, 423.
19 T. T. N. Do, T. V. Phi, T. P. Nguy, P. Wagner, K. Eersels, M. C. Vestergaard, L. T. N. Truong, *J. Electron. Mater.* **2017**, *46*, 3542.
20 D. Fan, N. Li, H. Ma, Y. Li, L. Hu, B. Du, Q. Wei, *Biosens. Bioelectron.* **2016**, *85*, 580.
21 Z. Biniaz, A. Mostafavi, T. Shamspur, M. Torkzadeh-Mahani, M. Mohamadi, *Microchim. Acta* **2017**, *184*, 2731.
22 M. Sajid, A. Osman, G. U. Siddiqui, H. B. Kim, S. W. Kim, J. B. Ko, Y. K. Lim, K. H. Choi, *Sci. Rep.* **2017**, *7*, 5802.
23 M. Roushani, A. Valipour, *Microchim. Acta* **2016**, *183*, 845.
24 J. Phair, L. Newton, C. McCormac, M. F. Cardosi, R. Leslie, J. Davis, *Analyst* **2011**, *136*, 4692.
25 A. Anderson, J. Phair, J. Benson, B. Meenan, J. Davis, *Mater. Sci. Eng., C* **2014**, *43*, 533.
26 T. J. Davies, R. G. Compton, *J. Electroanal. Chem.* **2005**, *585*, 63.
27 N. Godino, X. Borrisé, F. X. Muñoz, F. J. del Campo, R. G. Compton, *J. Phys. Chem. C* **2009**, *113*, 11119.

